The Effect of Titania Structure on Ni/TiO$_2$ Catalysts for *p*-Nitrophenol Hydrogenation*

CHEN Rizhi(陈日志)[a], **DU Yan**(杜艳)[b], **XING Weihong**(邢卫红)[a] **and XU Nanping**(徐南平)[a,**]

[a] College of Chemistry and Chemical Engineering, Nanjing University of Technology, Nanjing 210009, China
[b] College of Urban Construction and Safety & Environmental Engineering, Nanjing University of Technology, Nanjing 210009, China

Abstract The catalytic hydrogenation of *p*-nitrophenol to *p*-aminophenol was investigated over Ni/TiO$_2$ catalysts prepared by a liquid-phase chemical reduction method. The catalysts were characterized by inductively coupled plasma (ICP), X-ray powder diffraction (XRD), transmission electron microscopy (TEM), X-ray photoelectron spectra (XPS) and temperature-programmed reduction (TPR). Results show that the titania structure has favorable influence on physio-chemical and catalytic properties of Ni/TiO$_2$ catalysts. Compared to commercial Raney nickel, the catalytic activity of Ni/TiO$_2$ catalyst is much superior, irrespective of the titania structure. The catalytic activity of anatase titania supported nickel catalyst Ni/TiO$_2$(A) is higher than that of rutile titania supported nickel catalyst Ni/TiO$_2$(R), possibly because the reduction of nickel oxide to metallic nickel for Ni/TiO$_2$(A) is easier than that for Ni/TiO$_2$(R) at similar reaction conditions.

Keywords *p*-nitrophenol, catalytic hydrogenation, *p*-aminophenol, Ni/TiO$_2$ catalyst

1 INTRODUCTION

p-Aminophenol is an important intermediate in the preparation of analgesic and antipyretic drugs[1—7]. In order to meet the growing demand for *p*-aminophenol, direct catalytic hydrogenation of *p*-nitrophenol to *p*-aminophenol becomes important, because this could be an efficient and greener route[7]. Raney nickel[8], nano-sized nickel[9] and several noble metal catalysts such as Pd/C[7] have been used as catalysts for this reaction. Due to cheaper price and higher catalytic activity, supported nickel catalysts are widely used in various reactions[10—16]. Moreover, compared to unsupported nano-sized nickel catalysts, the supported nickel catalysts are easy to recover in a slurry reactor. There are few reports on the catalytic hydrogenation of *p*-nitrophenol over supported nickel catalysts.

Titania has attracted much interest as a support material for metals or metal oxides due to its ability to modify the catalytic properties of the supported phase[17,18]. It is known that titania exists in three main structures: anatase, rutile, and brookite, and each structure shows different physical properties. It is inferred that metal supported on titania with different structures might exhibit different physio-chemical properties and catalytic properties. However, little on such difference has been reported[19].

Therefore, in this work, we have attempted the catalytic hydrogenation of *p*-nitrophenol to *p*-aminophenol over Ni/TiO$_2$ catalysts. The catalysts were prepared by liquid-phase chemical reduction and characterized by inductively coupled plasma (ICP), X-ray powder diffraction (XRD), transmission electron microscopy (TEM), X-ray photoelectron spectra (XPS) and temperature-programmed reduction (TPR). The effects of titania structure (rutile and anatase) on the properties and catalytic activity of Ni/TiO$_2$ catalyst were studied. At the same time, the catalytic activity of Ni/TiO$_2$ catalyst was compared to that of commercial Raney nickel.

2 EXPERIMENTAL

2.1 Catalyst preparation

A series of Ni/TiO$_2$ samples were prepared by the liquid-phase chemical reduction method as follows. 10g TiO$_2$ (Nanjing Titanium Dioxide Chemical Co., average size 350nm, surface area 9m$^2 \cdot$g^{-1}) calcined in stagnant air at 500℃ for 4h was impregnated with 45ml NiSO$_4$ aqueous solution with different nickel ion concentration for 8h under low magnetic stirring. Then it was dried at 110℃ with gentle stirring overnight to exclude residual water. 5g precursor was reduced by adding 8ml hydrazine hydrate (N$_2$H$_4 \cdot$H$_2$O) solution, during which the mole ratio of N$_2$H$_4 \cdot$H$_2$O to Ni^{2+} was controlled at 2∶1 and the mixture was vigorously stirred. The resulting Ni/TiO$_2$ catalyst was washed with distilled water, followed by ethanol, and then dried in oven at 80℃. The nickel content in all cases was analyzed by inductively coupled plasma spectrophotometry (ICP, Optima 2000DV, PerkinElmer, USA) after extraction with nitric acid. The catalyst code used is *x*Ni/support, in which *x* is the actual

---

nickel loading (%, by mass).

2.2 Catalyst characterization

XRD patterns were obtained on a Bruker D8 instrument with Ni-filtered Cu K_α radiation (λ=0.154nm) at 40kV and 30mA, employing a scanning rate of $0.05°\cdot s^{-1}$ in the 2θ range from 30° to 80°.

The morphology and particle size of the supported nickel were observed by high-resolution transmission electron microscopy (HRTEM, JEM-2010). Specimens for HRTEM observations were sonicated in ethanol for 10min and then loaded onto a copper fine gauze with carbon coatings.

XPS were obtained in an ESCALAB MK II system with a base pressure of 1×10^{-9}kPa. Mg K_α radiation source ($h\nu$=1253.6eV) was used in XPS measurements. The C_{1s} signal (285eV) was taken as the reference to calculate the binding energies.

TPR was carried out in a quartz U-tube reactor, and 100mg sample was used for each measurement. Prior to the reduction, the sample was pretreated in a N_2 stream at 100℃ for 30min and then cooled to room temperature. After that, the H_2/Ar mixture (10% H_2 by volume) was switched on and the temperature was raised from 30℃ to 800℃ at a rate of $10℃\cdot min^{-1}$. The consumption of H_2 in the reactant stream was detected by a thermal conductivity cell.

2.3 Catalytic activity measurement

The catalytic hydrogenation of *p*-nitrophenol to *p*-aminophenol was carried out in a 300ml stainless steel autoclave equipped with a magnetically driven impeller. After definite amounts of catalysts and 14g *p*-nitrophenol in 163ml ethanol solution were introduced into the autoclave, it was sealed and purged with hydrogen for five times to purge the air. The reactor was then heated to a desired temperature under low stirring ($80r\cdot min^{-1}$). After the temperature reached the set value, hydrogen gas was introduced into the reactor to a set level, and the contents were stirred at $320r\cdot min^{-1}$. Last, the hydrogenation reaction was performed at 102℃ and 1.65MPa. The products were analyzed by a HPLC system (Agilent 1100 Series, USA) equipped with a diode array detector (DAD) and an auto-sampler. Chromatographic separations were performed at 35℃ using a ZORBAX Eclipse XDB-C18, 5μm, 4.6mm×250mm column. A mobile phase composed of 80% methanol and 20% water at a flow rate of $1ml\cdot min^{-1}$ was used.

3 RESULTS AND DISCUSSION
3.1 Catalyst characterization

Figure 1 shows the XRD patterns of a series of Ni/TiO$_2$(R) samples with different Ni loadings, and the result of TiO$_2$(R) is also presented for comparison. For the samples with low Ni loadings, *i.e.*, 5%, 10%, 15% and 20% in Ni/TiO$_2$(R), no characteristic peaks

of crystalline Ni can be observed, as shown in patterns (b), (c), (d) and (e). For the sample 30Ni/TiO$_2$(R), pattern (f), the characteristic peak of crystalline Ni (typically with 2θ=44.5°) marked by Miller index (1 1 1) is just observed. The results indicate that Ni is highly dispersed on the surface of rutile titania support. The XRD patterns of TiO$_2$(A) and a series of Ni/TiO$_2$(A) samples with different Ni loadings are shown in Fig.2. For the samples with low Ni loadings of 5% and 10% in Ni/TiO$_2$(A), also no characteristic peaks of crystalline Ni can be observed, as shown in patterns (b) and (c). It is interesting to find, for the anatase titania supported nickel catalyst, as Ni loading is 15%, the characteristic peak of crystalline Ni (typically with 2θ=44.5°) marked by Miller index (1 1 1) has been observed, as shown in pattern (d). As shown by comparison between patterns (d), (e) and (f), the intensity of characteristic peak of crystalline Ni increases with the Ni loading. These results show that the titania structure has great influence on the dispersion of loaded Ni, and the dispersion of Ni on the surface of rutile titania support is better than that on the surface of anatase titania support.
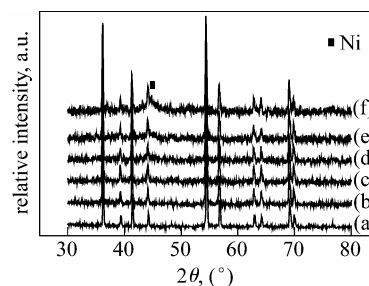

Figure 1   XRD patterns of the samples
(a) TiO$_2$(R); (b) 5Ni/TiO$_2$(R); (c) 10Ni/TiO$_2$(R);
(d) 15Ni/TiO$_2$(R); (e) 20Ni/TiO$_2$(R); (f) 30Ni/TiO$_2$(R)
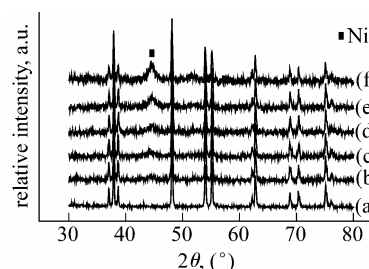

Figure 2   XRD patterns of the samples
(a) TiO$_2$(A); (b) 5Ni/TiO$_2$(A); (c) 10Ni/TiO$_2$(A);
(d) 15Ni/TiO$_2$(A); (e) 20Ni/TiO$_2$(A); (f) 30Ni/TiO$_2$(A)

The TEM micrograph of 20Ni/TiO$_2$(R) shown in Fig.3 indicates the Ni particles (dark field) are uniformly dispersed on the surface of rutile titania support. As observed from TEM, the average particle size of Ni is about 15nm. Fig.4 shows the TEM micrograph of 20Ni/TiO$_2$(A) indicating that the average particle size of Ni is about 30nm, clearly larger than that of Ni supported on rutile titania support, in accord to the XRD characterization.
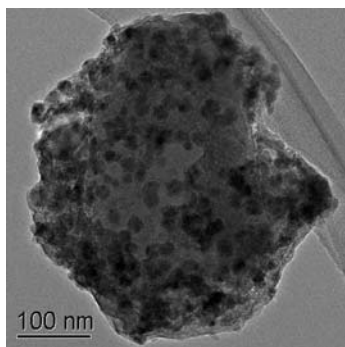
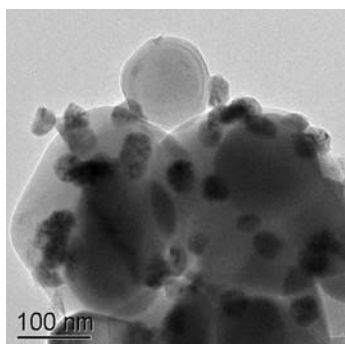**Figure 3   TEM micrograph of 20Ni/TiO₂(R) catalyst**

Figure 4   TEM micrograph of 20Ni/TiO₂(A) catalyst

The binding energy and surface Ni/Ti atomic ratio data are listed in Table 1. The binding energies of $Ni_{2p3/2}$ show that the surface of the samples are oxidized completely for both 20Ni/TiO₂(R) and 20Ni/TiO₂(A)[20]. It is obviously seen from Table 1 that the surface Ni/Ti atomic ratio for rutile titania supported nickel catalyst 20Ni/TiO₂(R) is much higher than that for anatase titania supported nickel catalyst 20Ni/TiO₂(A). This can been explained as follows: the ratio of titania surface covered by Ni for 20Ni/TiO₂(R) is higher than that for 20Ni/TiO₂(A), as clearly shown in Figs.3 and 4, hence, the Ni atoms detected by XPS at certain surface area of titania support for 20Ni/TiO₂(R) are more than that for 20Ni/TiO₂(A), that is to say, the surface Ni/Ti atomic ratio for 20Ni/TiO₂(R) is higher.

Table 1   XPS results of surface elements of catalysts

Catalysts	Binding energy of $Ni_{2p3/2}$, eV	Surface Ni/Ti atomic ratio
20Ni/TiO₂(A)	855.3	1.81
20Ni/TiO₂(R)	855.6	3.67

Figure 5 shows the TPR profiles for TiO₂(A), TiO₂(R), 20Ni/TiO₂(A) and 20Ni/TiO₂(R). As to the TiO₂(A) and TiO₂(R) samples, no evident H₂ consumption can be observed at temperatures lower than 800℃, as shown in profiles (a) and (b). The reduction profile of 20Ni/TiO₂(A) shows a broad hydrogen consumption pattern between 130℃ and 600℃. The reduction at low temperature may be ascribed to the

reduction of Ni₂O₃, which was also found for 10Ni/TiO₂ and 20Ni/TiO₂ catalysts as described by van de Loosdrecht *et al.*[18]. The reduction at high temperature from 260℃ to 600℃ is probably due to the reduction of bulk NiO and NiO with significant interaction with the titania surface[21]. The reduction peaks of 20Ni/TiO₂(R) have basic similar profile with those of 20Ni/TiO₂(A). However, the reduction of 20Ni/TiO₂(R) sets in at 160℃ and the peak maximum of low-temperature reduction peak is at 223℃, which are all at higher temperature than observed for 20Ni/TiO₂(A). The results are indicative of stronger interaction between Ni and titania support for 20Ni/TiO₂(R). Comparing the profiles (c) and (d), it can be found that the reduction peaks area of 20Ni/TiO₂(R) is obviously larger than that of 20Ni/TiO₂(A), which means that the oxidation degree of Ni supported on rutile titania is comparatively higher. These results indicate, compared to 20Ni/TiO₂(R), the reduction of nickel oxide to metallic nickel for 20Ni/TiO₂(A) is easier. TPR results show the existence of nickel oxide on the surface of Ni/TiO₂, which is also revealed by XPS characterization.
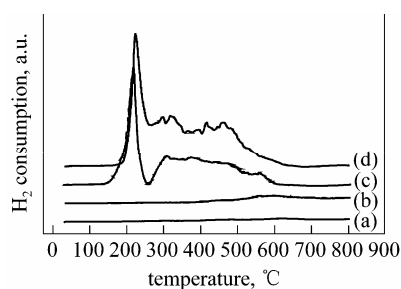

Figure 5   TPR profiles of the samples
(a) TiO₂(A); (b) TiO₂(R); (c) 20Ni/TiO₂(A); (d) 20Ni/TiO₂(R)

3.2   Catalytic activity

The preliminary experiments on the hydrogenation of *p*-nitrophenol indicate that no hydrogenation reaction occurs in the absence of the catalyst, which confirms the absence of any noncatalytic reaction. Moreover, at a fixed temperature, the partial pressure of solvent ethanol-water also remains constant. So, the decrease of pressure in the reactor with time is caused only by catalytic hydrogenation of *p*-nitrophenol to *p*-aminophenol. Therefore, the catalytic activity could be expressed by reaction rate defined as the amount of hydrogen consumed per minute and per liquid phase volume.

Figure 6 shows the change of reaction rate with time, with 20Ni/TiO₂(A) and 20Ni/TiO₂(R) as catalyst, respectively, and for the sake of comparison, the result of Raney nickel (average size 330μm, surface area 71m²·g⁻¹) provided by Anhui Bayi Chemical Co. is also presented. The reaction rate of the hydrogenation over as-prepared Ni/TiO₂ catalyst first increases with time, then becomes stabilized, and then decreases. The first stage corresponds to the activation of Ni/TiO₂.

The second and third stages are related to the concentration of p-nitrophenol[7,9], namely that the reaction rate is not affected by p-nitrophenol concentration except when the conversion of p-nitrophenol is high. The end conversion of p-nitrophenol is (a) 16.5%, (b) 99.9% and (c) 99.9% respectively. Compared to Raney nickel, as-prepared Ni/TiO$_2$ catalyst has higher catalytic activity, irrespective of the titania structure, at similar reaction conditions. For an example, the reaction rate of 20Ni/TiO$_2$(A) is about 10 times higher than that of Raney nickel. It is worth noting that the catalytic activity of anatase titania supported nickel catalyst 20Ni/TiO$_2$(A) is higher than that of rutile titania supported nickel catalyst 20Ni/TiO$_2$(R).
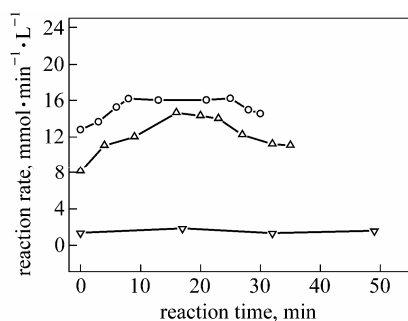

Figure 6   Reaction rate of p-nitrophenol hydrogenation over various catalysts
▽ 0.3g Raney nickel; △ 1.67g 20Ni/TiO$_2$(R);
○ 1.67g 20Ni/TiO$_2$(A)

Combined with the foregoing results from XRD and TEM, we can find that the catalytic activity of 20Ni/TiO$_2$ cannot be correlated with the usual criteria of metal dispersion and particle size; on the contrary, the higher the nickel dispersion and smaller the particle size, the lower the catalytic activity. According to the results of TPR shown in Fig.5, it may be concluded that the stronger metal-support interaction for 20Ni/TiO$_2$(R) makes the reduction of nickel oxide to metallic nickel more difficult compared to 20Ni/TiO$_2$(A) at similar reaction conditions, and as a result, the amount of metallic nickel for 20Ni/TiO$_2$(R) is less, and the catalytic activity of 20Ni/TiO$_2$(R) is lower. Rode $et\ al.$[22] also found that the catalytic activity was higher for the supported nickel catalyst having a smaller degree of nickel dispersion in the gas-phase hydrogenation of benzonitrile and acetonitrile. They suggested that the surface geometry of nickel particles was of importance for the catalytic activity. As shown in Fig.7, the catalytic activities (expressed as the reaction rate at 20min) of Ni/TiO$_2$(A) are all higher than those of Ni/TiO$_2$(R) with different Ni loadings. Within the experimental range, with an increase of nickel loading, the catalytic activity of Ni/TiO$_2$(A) gradually increases while the catalytic activity of Ni/TiO$_2$(R) first increases and then changes slightly, possibly because of the higher nickel dispersion for Ni/TiO$_2$(R) compared to Ni/TiO$_2$(A), as a result with respect to

Ni/TiO$_2$(R) the nickel particles would agglomerate at a lower nickel loading. These results indicate that Ni/TiO$_2$(A) is a better catalyst for the catalytic hydrogenation of p-nitrophenol to p-aminophenol.
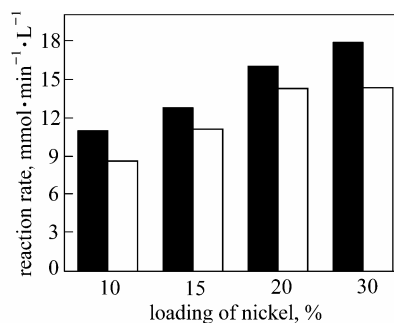

Figure 7   Reaction rate of p-nitrophenol hydrogenation over Ni/TiO$_2$(A) and Ni/TiO$_2$(R) with different nickel loadings (catalyst, 1.67g)
■ Ni/TiO$_2$(A);   □ Ni/TiO$_2$(R)

4   CONCLUSIONS

A series of Ni/TiO$_2$ catalysts were prepared by the liquid-phase chemical reduction method. The results of catalyst characterization show that the titania structure has significant influence on the dispersion, particle size and reduction behavior of titania supported nickel catalyst. The catalytic hydrogenation of p-nitrophenol to p-aminophenol was investigated over Ni/TiO$_2$ catalysts in a laboratory-scale batch-slurry reactor. The catalytic activity of as-prepared Ni/TiO$_2$ catalyst is much superior over that of commercial Raney nickel. Compared to Ni/TiO$_2$(A), the catalytic activity of Ni/TiO$_2$(R) is lower, which is not correlated with the usual criteria of metal dispersion and particle size; on the contrary, the higher the nickel dispersion and smaller the particle size, the lower the catalytic activity. This may be because the reduction of nickel oxide to metallic nickel for Ni/TiO$_2$(A) is easier than that for Ni/TiO$_2$(R) at similar reaction conditions.

REFERENCES

1   Rode, C.V., Vaidya, M.J., Jaganathan, R., Chaudhari, R.V., "Hydrogenation of nitrobenzene to p-aminophenol in a four-phase reactor: reaction kinetics and mass transfer effects", $Chem.\ Eng.\ Sci.$, **56**, 1299—1304(2001).
2   Rode, C.V., Vaidya, M.J., Chaudhari, R.V., "Synthesis of p-aminophenol by catalytic hydrogenation of nitrobenzene", $Org.\ Process\ Res.\ Dev.$, **3**, 465—470(1999).
3   Komatsu, T., Hirose, T., "Gas phase synthesis of $para$-aminophenol from nitrobenzene on Pt/zeolite catalysts", $Appl.\ Catal.\ A$: $Gen.$, **276**, 95—102(2004).
4   Sathe, S.S., "Process for preparing p-aminophenol in the presence of dimethyldodecylamine sulfate", US Pat., 4176138(1979).
5   Lee, L.T., Chen, M.H., Yao, C.N., "Process for manufacturing p-aminophenol", US Pat., 4885389(1989).
6   Yun, K.S., Cho, B.W., "Process for preparing $para$-aminophenol", US Pat., 5066369(1991).
7   Vaidya, M.J., Kulkarni, S.M., Chaudhari, R.V., "Synthesis of p-aminophenol by catalytic hydrogenation of p-nitrophenol",

Org. Process Res. Dev., **7**, 202—208(2003).

8 Chen, R.Z., Du, Y., Chen, C.L., Xing, W.H., Xu, N.P., Chen, C.X., Zhang, Z.L., "Comparative study on catalytic activity and stability of nano-sized nickel and Raney nickel", *J. Chem. Ind. Eng. (China)*, **54**, 704—706(2003). (in Chinese)

9 Du, Y., Chen, H.L., Chen, R.Z., Xu, N.P., "Synthesis of *p*-aminophenol from *p*-nitrophenol over nano-sized nickel catalysts", *Appl. Catal. A: Gen.*, **277**, 259—264(2004).

10 Rautanen, P.A., Aittamaa, J.R., Krause, A.O.I., "Liquid phase hydrogenation of tetralin on Ni/Al₂O₃", *Chem. Eng. Sci.*, **56**, 1247—1254(2001).

11 Suh, D.J., Park, T.J., Lee, S.H., Kim, K.L., "Nickel-alumina composite aerogels as liquid-phase hydrogenation catalysts", *J. Non-Cryst. Solids*, **285**, 309—316(2001).

12 Wu, W.H., Xu, J., "Liquid-phase hydrodechlorination of chlorinated benzenes over active carbon supported nickel catalysts under mild conditions", *Catal. Commun.*, **5**, 591—595(2004).

13 Wu, W.H., Xu, J., Ohnishi, R., "Complete hydrodechlorination of chlorobenzene and its derivatives over supported nickel catalysts under liquid phase conditions", *Appl. Catal. B: Environ.*, **60**, 129—137(2005).

14 Kapoor, M.P., Matsumura, Y., "A comparative study of liquid- and gas-phase methanol decomposition catalyzed over nickel supported on silica", *J. Mol. Catal. A: Chem.*, **178**, 169—172(2002).

15 Toppinen, S., Rantakylä, T.K., Salmi, T., Aittamaa, J., "The liquid phase hydrogenation of benzene and substituted alkylbenzenes over a nickel catalyst in a semi-batch reactor", *Catal. Today*, **38**, 23—30(1997).

16 Quincoces, C.E., González, M.G., "Kinetic study on CO₂ reforming of methane", *Chin. J. Chem. Eng.*, **9**, 190—195(2001).

17 Hadjiivanov, K., Mihaylov, M., Abadjieva, N., Klissurski, D., "Characterization of Ni-TiO₂ catalysts prepared by successive adsorption-reduction of Ni²⁺ ions", *J. Chem. Soc., Faraday Trans.*, **94**, 3711—3716(1998).

18 van de Loosdrecht, J., van der Kraan, A.M., van Dillen, A.J., Geus, J.W., "Metal-support interaction: titania-supported and silica-supported nickel catalysts", *J. Catal.*, **170**, 217—226(1997).

19 Li, Y.Z., Xu, B.L., Fan, Y.N., Feng, N.Y., Qiu, A.D., Miao, J.W., He, J., Yang, H.P., Chen, Y., "The effect of titania polymorph on the strong metal-support interaction of Pd/TiO₂ catalysts and their application in the liquid phase selective hydrogenation of long chain alkadienes", *J. Mol. Catal. A: Chem.*, **216**, 107—114(2004).

20 Zheng, H.G., Liang, J.H., Zeng, J.H., Qian, Y.T., "Preparation of nickel nanopowders in ethanol-water system (EWS)", *Mater. Res. Bull.*, **36**, 947—952(2001).

21 Ho, S.W., Chu, C.Y., Chen, S.G., "Effect of thermal treatment on the nickel state and CO hydrogenation activity of titania-supported nickel catalysts", *J. Catal.*, **178**, 34—48(1998).

22 Rode, C.V., Arai, M., Shirai, M., Nishiyama, Y., "Gas-phase hydrogenation of nitriles by nickel on various supports", *Appl. Catal. A: Gen.*, **148**, 405—413(1997).